2018

An investigation on pipe surface topography beyond roughness

Sebastian, E.

Sebastian, E. (2018) 'An investigation on pipe surface topography beyond roughness', The Plymouth Student Scientist, 11(1), p. 170-198.
http://hdl.handle.net/10026.1/14177

The Plymouth Student Scientist
University of Plymouth

*The Plymouth Student Scientist, 2018, **11** (1), 170-198*

An investigation on pipe surface topography beyond roughness

Emil Sebastian

Project Advisor: Daniel Hatton, School of Engineering, Plymouth University, Drake Circus, Plymouth, PL4 8AA

Abstract

There are always problems with pipes and associated blockages. These problems are commonly due to the obstacles sitting inside the pipe, such as sand particles and pebbles. This study considers whether there is any effect of topographies on pipe flow and how big the effect is, and to determine the characteristics of the topographies that affect the flow. The study was conducted by designing two types of topographies with similar shape but with different dimensions and spacing (wavelength) between asperities, Topography-1 and Topography-2. The study used a traditional experimental method. Topography was made by a casting process; firstly, by designing the topography and its mold using a Computer Aided Design (CAD) software and then creating the mold to cast the topography. Testing was conducted outdoors, inserting the rubber topographic component into a 110mm drainage pipe and then using a submersible pump to propel water through the pipe, with flow controlled using a valve in each set of the test. Testing was done by pumping water from a filled tank to an empty tank, using a plain pipe first; and then on two separate types of topography, enabling a subsequent analysis of the effects of the pipe on water flow with and without the topographic surface. The results were then processed to determine the flow rate, Reynolds number and Euler number as the water flows through the pipe. Statistical error calculations were performed to see how the results met the expectations of accuracy. Results from the experiment showed that there was an effect on the flow characteristics when water flowed through the topographic surface compared to the plain pipe. Topography-2 had a bigger effect on the pipe flow compared to Topography-1. Topopography-2 had a larger surface area compared to Topgraphy-1.

1. Table of contents

2. Nomenclature

A	Cross sectional area of the inner surface of the pipe.
D	Hydraulic diameter of the pipe
E	Evidence
E_u	Euler Number
H	Theoretical Model
ΔH_w	Water height level difference in the tank
ID	Inner diameter of the test pipe
L	Length of the pipe
MDF	Medium Density Fibreboard
N	Number of test runs
OD	Outer diameter of the test pipe
Q	Flow rate
Re	Reynolds Number
V	Volume of the tank
V_{error}	Random error in Volume
b_t	Breadth of the tank
d.p	Decimal place
g	Acceleration due to gravity
h	Set of values
Δh	Head difference
l_t	Length of the tank
m	Mean variable value from the number of test runs
t	Time taken to reach the pre-set water level difference
t_{error}	Random error in time
x_i	Individual variable value
Σ	Sum of all
ϵ	Relative roughness
λ	Darcy friction factor
μ	Dynamic Viscosity
ρ	Density of water
φ	Random Error
$\frac{\partial Re}{\partial V}$	Small change in Reynolds number with respect to Volume
$\frac{\partial Re}{\partial t}$	Small change in Reynolds number with respect to small change in time

3. List of figures

4. List of tables

(Appendix 14)

5. Introduction

This project researched and tested different topographies inside a pipe to see how they affected flow characteristics such as flow rate, velocity, Reynolds number and difference in pressure due to head difference. Different topographies have an effect on change in friction which affects the flow behaviour inside the pipe. Researchers such as Darcy in 1857, Weisbach in 1845, Moody in 1944 and Nikuradse in 1933 have done similar types of study on flow characteristics in the pipe flow (Brown 2003). Conducting study on this will help to design suitable pipe for different manufacturing industries as they need different types of flow behaviour for their product manufacturing (Kalyanaraman 2012). Chocolate factories, for example, need smooth and laminar flow to avoid swirling and bubbling as this will misshape the chocolate bars so that the company should make sure that the duct or pipe through which the chocolate flows should be as smooth as possible (Chapman 2008). However, turbulent flow is good for mixing different fluids and will be useful for making anything related to mixing different fluids (Chapman 2008). This study can be applied in gas and oil industry; as water, oil and gas are fluids and if Mach number is irrelevant theses fluids are dynamically similar when Reynolds number is same in them (Faber 1995).

6. Aims

1. To enable improved and informed choice of desirable pipe topography to provide constant flow rate everywhere with less pressure for energy saving.
2. To predict the least amount of pressure needed to drive the water flow through water supply pipe.
3. To measure the variation in time it will take for the water flowing as the intensity and dimensions of the topographies changes.

7. Objectives

1. Designing a surface topography that have same roughness like traditional method that Nikuradse in 1933 conducted but with different shape and wavelength.
2. Design two topographies with varying spacing (wavelength) between asperities for controlled topographic surfaces.
3. Design and manufacture casting method for creating these topographies
4. The pressure difference across the pipe can be measured by installing pressure gauges across the pipe. This will be helpful to know the relation between the pressure loss and the Reynolds number of the water flowing through different topographies.
5. Measuring the pressure gradient and flow rate as the flow proceeds through the topographies to see how the variables get affected.

8. Literature review

8.1. Effect of topographies on the pipe inner surface

The term surface roughness is frequently regarded as a similar meaning with surface texture and surface topographies (Smith 1994). Therefore, it is assumed that different topographies inside the pipe are sometimes considered as just the different roughness, however there is more to topographies than roughness (Smith 1994). Roughness is said to be the relative roughness which is just the peak height of the rough layer inside the pipe (Afzal 2007). Whereas topography can be in any shape, size and number as in this experiment, the spacing between each

topographic asperity varies, therefore topographies have further effects on the water flow characteristics when the water flows through the topographic pipe. Roughness only deals with the height of the textured layer, whereas topography deals with length to diameter ratio, flow connections, shape of the topography and wave length of the topographies. Therefore, roughness and topography is different. This paper does not provide a separate detailed definition of topography rather than relating to the surface roughness. The fully developed turbulent flow behaviour can be measured in the range of Reynolds numbers between 57×10^3 and 21×10^6 where the flow produces smooth, transitionally rough and fully rough flow behaviour (Shockling, Allen & Smits 2006).

Reynolds number is a dimensionless group that is proportional to inertial force divided by viscous force (Batchelor 1955). It can be analysed to determine which type of flow behaviour a fluid will show when there is substantial velocity gradient (Batchelor 1955). The roughness in the pipe wall has a great effect on the frictional loss and the loss on pump head varies by square of the flow velocity.

The friction factor of turbulent flow in the pipes can be calculated using the formula ${}^{1}/_{\sqrt{\lambda}} = 1.14 - 2\log_{10}\left(\frac{e}{D} + \frac{9.35}{Re\sqrt{\lambda}}\right)$ for Re> 4000 (Sonnad & Goudar 2007).

The Darcy-Weisbach equation and the content in the Moody chart only applies in a fully developed flow region so it is important that the flow that is being studied is fully developed (Mills 1992). A Moody chart is used to determine the Darcy friction factor when the Reynolds number and pipe roughness is known (Clifford et al. 2006). A Moody chart is shown in Figure-34 in Appendix-18. The Darcy Weisbach equation is

$\Delta h = \lambda \frac{L}{D} \frac{u^2}{2g}$ where Δh is head difference, λ is Darcy friction factor, L is the length of the pipe, D is the hydraulic diameter of the pipe, u is the velocity of the flow and g is the acceleration due to gravity (Jones et al. 2008).

The turbulent flow in the presence of surface roughness, the topography is often represented by a characteristic roughness height k which might be taken as the root-mean- squared roughness height k_{rms} as the mean of the modulus of height from a perfectly cylindrical surface (Shockling, Allen & Smits 2006). Roughness due to different topographies on the pipe wall affects the pressure drop of the water flowing through that pipe. It constricts the flow area in the pipe and it also increases the wall shear stress (Kandlikar et al. 2015)). As the flow becomes turbulent flow the friction factor decreases as the velocity increases and once the velocity profile reaches the fully developed profile, the friction factor remains constant for all higher velocities (Judy, Maynes & Webb 2002).The wave length, skewness & kurtosis in the surface topography can affect the flow characteristics; the distinction between forms of topography includes waviness (Smith 1994). Wavelength, skewness and kurtosis are topographic properties of a surface that exist in addition to roughness, and that their effect on flow in the pipe is less well-studied than that of roughness.

8.2. Nikuradse's test on roughness

The factor f is the Darcy friction factor λ which is replaced by the Euler number in this project, Re is the Reynolds number of the water flow and p is the pressure difference across the length of the pipe. The Euler number is a flow characteristic that affects the pipe flow. The Euler number is said to be the ratio of the square root of inertial force to pressure force (Bansal 2001).

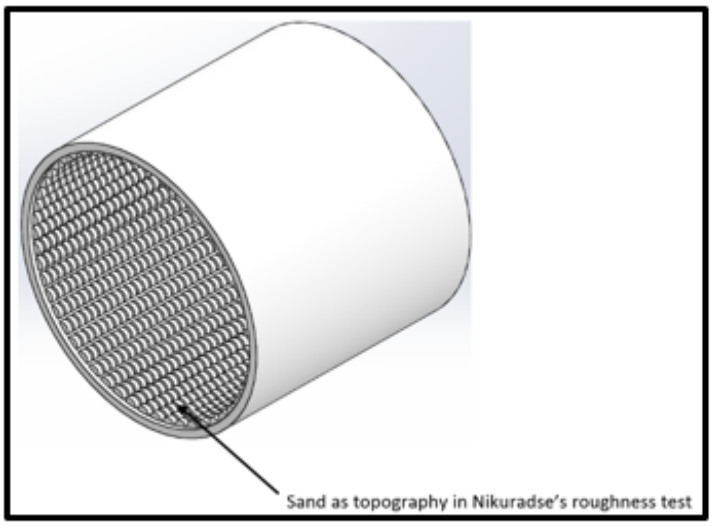

Figure-1: Explanatory diagram of Nikuradse's roughness test

The experiment in this project is similar to the "equivalent sand- grain roughness value" test done by Nikuradse. In Nikuradse's test it used sand as the topographic surface to create roughness for the fluid to flow past. The test involved series of pipes, sand grains with known size were glued on those pipe walls (Munson et al. 2010). The pressure drop needed to produce a desired flow rate was measured and the data were converted into friction factor for the corresponding Reynolds number and relative roughness (Munson et al. 2010). The data gained from the experiment showed, transitionally rough regime the friction factor gradually increasing above the smooth curve, reaching a minimum value before rising and levelling off to the fully developed rough value (Allen et al. 2007).

8.3. Components and materials

Detailed explanation of mold making and silicon rubber casting is shown in Appendix-3 and 8. The material used to create a mold for a topographic cast is Medium Density Fiberboard (MDF). MDF is a man-made wood composed of wood fiber bonded together with resin under heat and pressure (Kartal & Green 2002).

MDF has high strength and is easy to machine (Li et al. 2009), which means it can be machined to make a cylindrical slot on it to create a cylindrical topographic cast. MDF is readily available in stock and it is 9mm in depth which was acceptable.

The mold for the topography casting is created by laser cutting a 9mm deep cylindrical slot on the rectangular MDF sheet with dimensions of 900mm length and 299.39mm width which is the same as the inner circumference of the pipe. Laser cutting is highly

beneficial due its high machining precision and processing speed (Harimkar, Narendra & Sandip 2008).

Mold Max 30 silicon rubber solution is used as the cast material to create the topographic cast. The curing condition for this rubber solution is 24hours at 23℃ room temperature (Mold Max® 60 High Heat Resistant Silicone Rubber Compound 2017). An additional 4-5 hours at 51℃ will avoid any residual and alcohol that is a byproduct of the condensation reaction (Mold Max® 60 High Heat Resistant Silicone Rubber Compound 2017). A releasing agent can be applied on the rubber solution when cured to avoid sticking on to the cast when releasing (Mold Max® 60 High Heat Resistant Silicone Rubber Compound 2017). When cured and released from the cast the rubber solution will have designed topographies on the surface of it. The rubber solution will then fold around and insert into the pipe that will be used in the experiment. The plan was to use a OOMOO 30 Silicon rubber solution first which was readily available in stock but it pre-cured and became viscous. The casting process is shown in Figures-24 and 25 in Appendix- 8 and 9. Pipe material will be Polyvinyl Chloride (PVC). PVC pipes are light weight and available in any length (Chasis 1988). They are non- toxic material so they are safe to use, no risk in the range of conditions that will be encountered in these experiment (Chasis 1988). PVC pipes are quite cheap (Chasis 1988). PVC pipes are readily available in the workshop.

8.4. Pump

A submersible pump is used to pump water through the pipe; the submersible pump is arranged with an electric motor that is mounted in an appropriate water proof housing therefore the pump can be operated under water (Walshin 1960).

The operation of the submersible pump is controlled by various controlling systems such as float devices that submerge or float on the water tank (Walshin 1960). Movement of the float device in and out of the tank controls the starting and stopping of the pump mechanism (Walshin 1960). The pump starts operating when the float device is in the water tank and when the float device is taken off from the tank the submersible pump stops pumping the water (Walshin 1960). Figure-7 shows the water pumping into a tank, while Figure-8 shows the pump in use.

9. Methodology

9.1. Apparatus

- Plastic pressure tube 1.6m long x 2
- Ruler 1m long x 1
- Vertical timber board x 1
- Trolley x 1
- Pressure tap x 1
- Test Pipe 1.6m long x 1 (OD: 110mm & ID: 95.3mm)
- Topography x 2 (see Fig.4.1 & 4.2)
- Submersible pump x 1
- Pipe connecting pump to the test pipe x 1
- Pipe fitting plug x 1
- Pipe fitting coupler x 1
- Pipe tightener x 2
- Pipe valve x 1
- Tightening harness x 2

- Stopwatch x 1
- Action camera x 1
- Hand held action cam tripod x 1
- 1.1m x 0.91m rectangular tank x 2

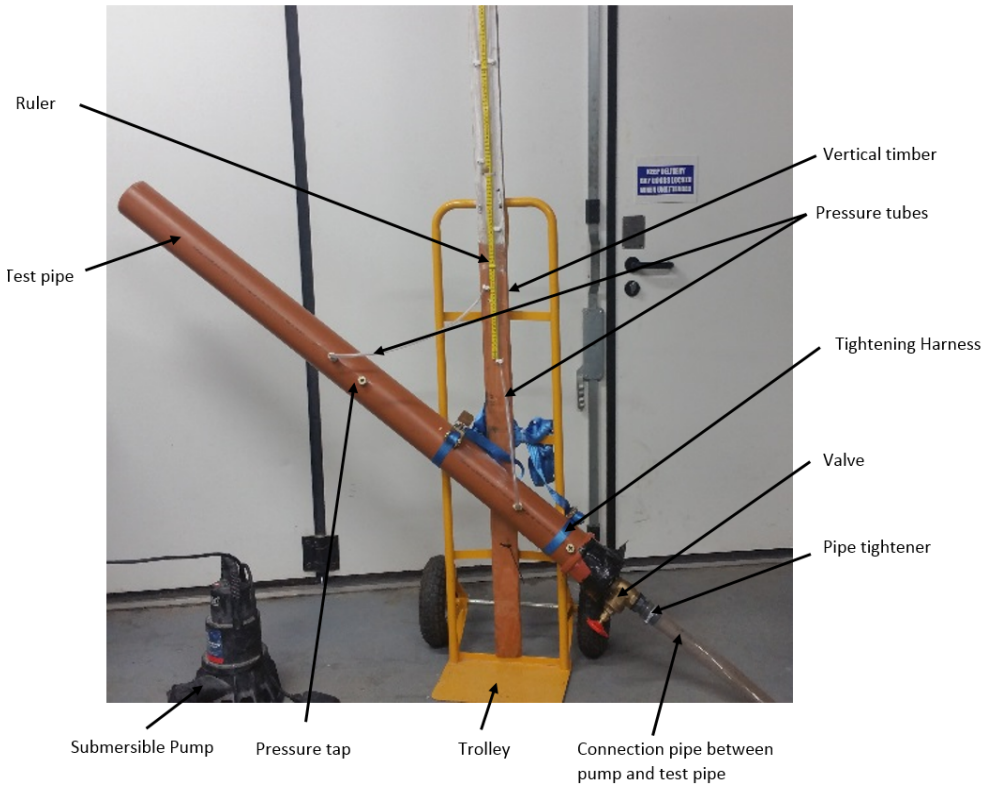

Figure-2: Apparatus

An open top manometer is used to measure the head difference across the pipe. An open top manometer has the same working principle as a piezometer. A piezometer consists of pressure tubes, as the water flows through the pipe connected with the piezometer the water will be forced up the pressure tube to some height (Hamill, 2011). This height is known as the piezometer head (Hamill, 2011). The open top manometer used here has two pressure tubes to measure the head difference upstream and downstream. An open-top manometer can compensate different hydraulic flow profiles such as flow angle as piezometer has this benefit (Liptak, 1993). Figure-4 shows the meniscus representing the head difference in an open top manometer. The time is measured using a stopwatch and the head difference is measured by video recording the movement of the meniscus in the pressure tube. The water level difference is observed on the ruler fixed on the tank wall.

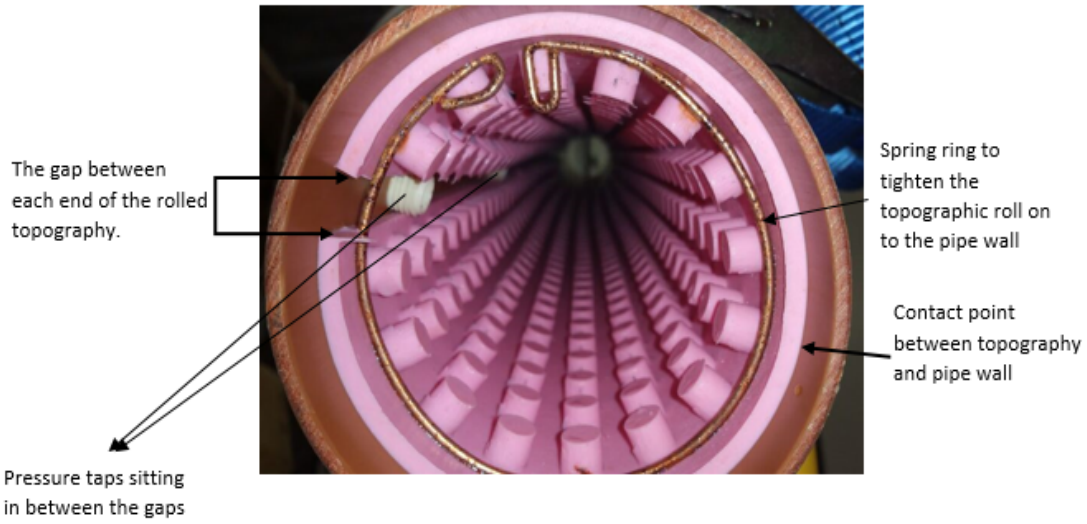

Figure-3: Topography fitted inside the test pipe

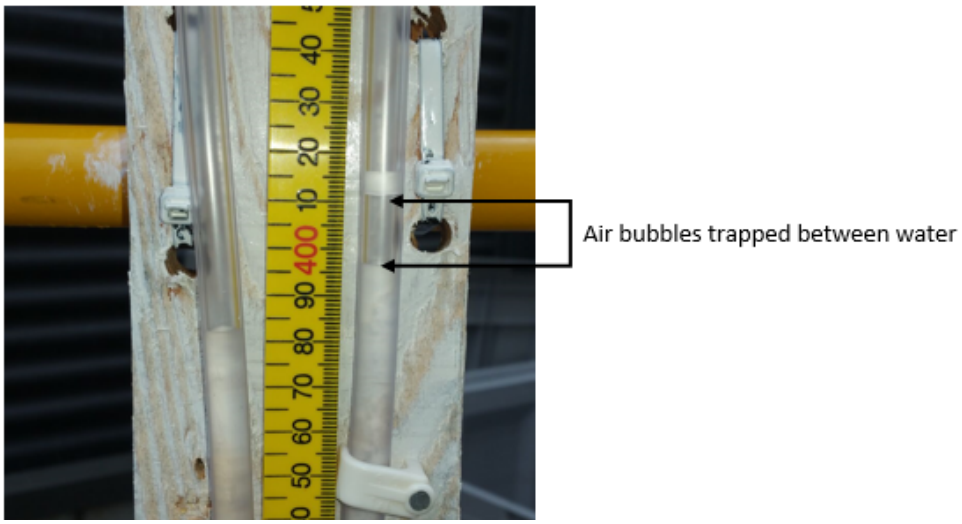

Figure-4: Head difference shown in the open top manometer

One pipe is used to test two types of topography, after testing one topography it is taken out and the other topography is inserted and then tested.

The detailed setting up of the apparatus and the topography insertion method is shown in Appendix-1.

Topography-1, shown in Figure 5, has 28 radial asperities and 59 in the longitudinal direction (total 1,652) whereas Topography-2, shown in Figure 6 has only 15 asperities in the radial, and 29 in the longitudinal, direction (total 435).

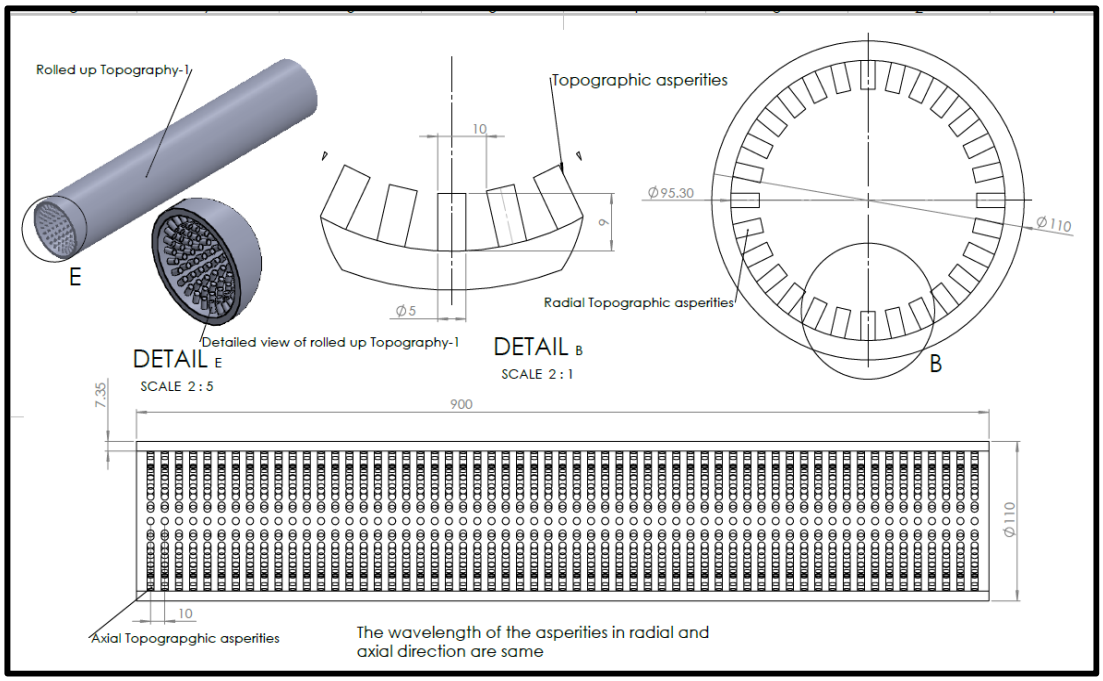

Figure-5: Topography-1 with its dimentions and spacing between each asperities labelled.

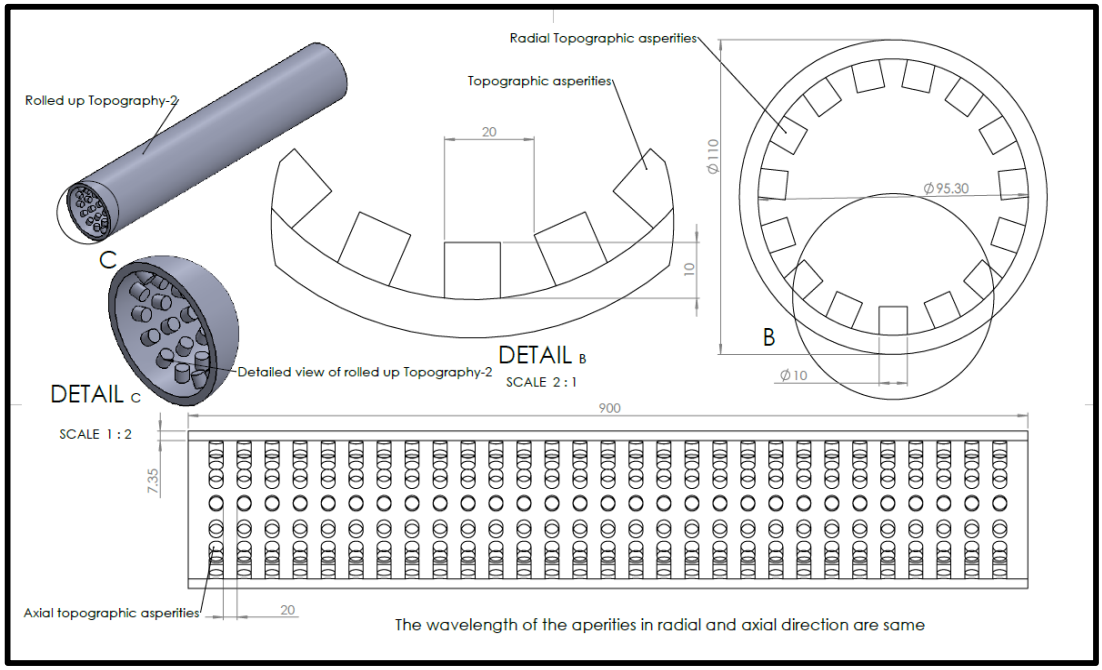

Figure-6: Topography-1 with its dimentions and spacing between each asperities labelled

Figure-7: Pumping water from Tank A to Tank B

Figure-8: Submersible pump placed inside the tank to start pumping

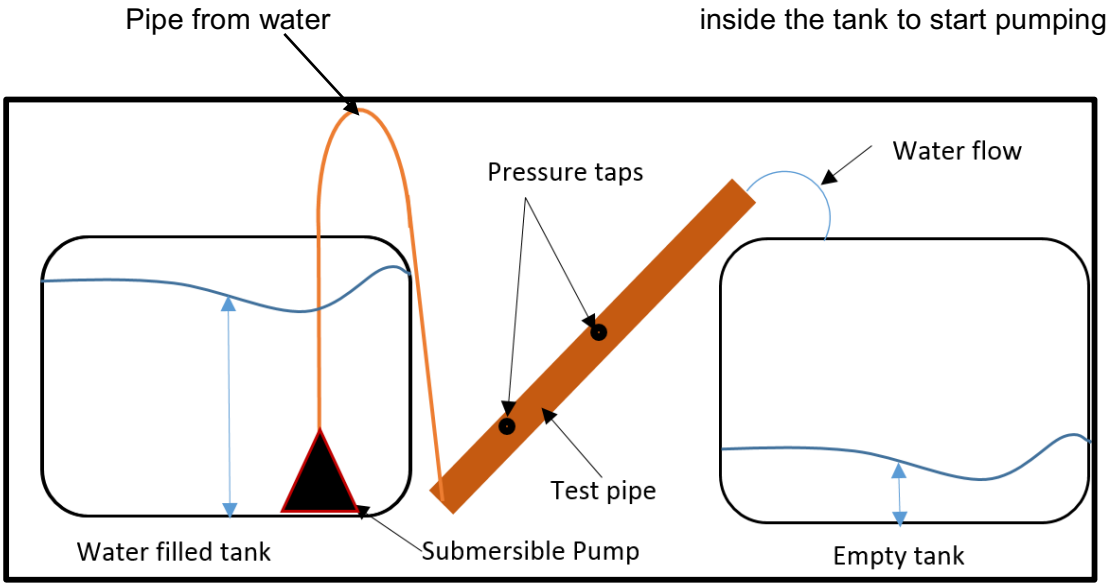

Figure-9: Schematic diagram of water pumping from full tank to empty tank.

The testing method involved two tanks, A and B; tank A was filled with water and tank B was empty. Each tank had a ruler that measured the water height level during the test, attached on its inside wall for volume measurement. The test model was positioned towards tank B, the test pipe pointing into tank B. A submersible pump was placed in tank A to pump water. Once tank A was empty the test model was brought towards tank A and the pump swapped into tank B to pump water to tank A. This swapping of pump and test model continued throughout the testing.

9.2. Theory

There are two theories behind this experiment, based on the Colebrook equation which is applied both when Topography-1 and 2 is same or where they are different. The Colebrook equation is represented by:

$$\frac{1}{\sqrt{\lambda}} = -2\log_{10}\left(\frac{\epsilon/D}{3.7} + \frac{2.51}{Re\sqrt{\lambda}}\right)$$

where Re is the Reynolds number, λ is the Darcy Friction factor, ϵ is the relative roughness inside the pipe and D is the hydraulic diameter of the pipe (Sonnad & Goudar 2007). In this project λ is replaced with its dimensionless variable called the Euler number because λ has velocity $\left(\frac{Q}{A}\right)$ in which the random error in velocity affects λ. The Reynolds number already has random error in it due to the presence of velocity in its equation. The Euler number equation is:

$\frac{\rho^2 D^3 g \Delta h}{2\mu^2 L}$ and a derivation of the Euler number involves the λ equation and the Reynolds number equation, as shown below:

$$Re = \frac{4\rho Q}{\pi \mu D} \quad 1$$

$$h_f = \lambda \frac{Lu^2}{D2g} \quad 2$$

$$u = \frac{Q}{A} = \frac{4Q}{\pi D^2}$$

$$h_f = \lambda \frac{Lu^2}{D2g} = \lambda \frac{64Q^2 L}{\pi^2 D^5 2g} = \lambda \frac{32Q^2 L}{\pi^2 D^5 g}$$

$$\lambda = \frac{h_f \pi D^5 g}{32Q^2 L} \quad 3$$

$$Q = Re\frac{\pi \mu D}{4\rho} \quad 4$$

$$\lambda = \frac{h_f \pi^2 D^5 g}{32Q^2 L} = \frac{h_f \pi^2 D^5 g}{32\frac{Re^2 \pi^2 \mu^2 D^2}{16\rho^2} L} = \frac{\rho^2 h_f D^3 g}{2Re^2 \mu^2 L}$$

$$\lambda = \frac{\rho^2 h_f D^3 g}{2Re^2 \mu^2 L} \quad 5$$

$$\lambda Re^2 = \frac{\rho^2 h_f D^3 g}{2\mu^2 L} = E_u$$

Colebrook's equation is then modified by replacing 2.51 value with constant A.

$\frac{\epsilon/D}{3.7}$ in the Colebrook's equation is replaced by the constant B because relative roughness and hydraulic diameter is the same for both Topography-1 and 2. Two sets of hypothetic models need to be considered, Model s and Model d. Model s is the hypothesis in which constants A and B have the same value for each topography and Model d is the hypothesis in which at least one constant value is different in each topography (Jeffreys 1961). The theory finds that the value of constants A and B for Topography-1 and 2 is same, or the value of constants A and B is separate for Topography and Topgraphy-2; and hence reveals whether Model s or Model d has the greatest probability. Colebrook's equation is then rearranged to make a Reynolds Number:

$$Re = -2\sqrt{E_u}\log_{10}\left(\frac{A}{\sqrt{E_u}} + B\right).$$

9.3. Methodology for results

The whole test was done in three sets; each set of tests was conducted by varying the flow of water and water level difference. For example, in Set 1 the valve controlling the water flow was closed to 6 full turns on the valve, in Set 2 the valve was opened to 1 turn from the 6 turn closed valve and in Set 3 the valve was opened to 2 turns from 6 turn closed valve. Set 1 measured the time it took to reduce the water height level by 10cm from the starting height level as the water got pumped to the empty tank. In the second set it was 20cm and in the third set it was 30cm. To increase the precision of the test result it was decided to do 3 runs on each set; for example, test set 1 (10cm): 1a,1b,1c; test set 2 (20cm): 2a,2b,2c and test set 3 (30cm): 3a,3b,3c; then took the average value from each run in the set (Squires 2001). The head difference was obtained by video recording the fluctuation of the meniscus. After recording the video, it was played on a computer to the numerical value. This method was performed for each topography and plain pipe testing. The plain pipe was a normal surface with no topography inserted. The reason why the valve was closed to 6 full turns was, when the valve was fully opened the meniscus was fluctuating highly and quickly; therefore, the valve was closed until the meniscus became stable or reduced the fluctuation close to stable. When the meniscus became close to stable, the number of times the valve was turned to close the valve to get a low fluctuating meniscus in the pressure tube was recorded. The first set of the test was then run with this number of turns and on the next set of the test the valve was opened to one turn each time from the stabilising point. On the 6th full turn of the valve the meniscus in the pressure tube reduced its fluctuation. Each set of the tests were also varied with the water level difference along with the varying flow of the water.

After obtaining results from the experiment, the standard deviation and standard error on each variable were calculated using equation-7 and 8 shown in Appendix-13. Those results were then processed to determine the flow rate of the water during each test run, hence determining the Reynolds number. With the head difference obtained the Euler number is determined. A graph of the Euler number against the Reynolds number was plotted based on the results from each test set on the plain pipe, Topography-1 and Topography-2 with the standard error bars shown to find the effect of the topographies on the pipe flow. To find the trend of the values of constants A and B in the Colebrook equation for Topographies-1 and 2, the Chi Squared Statistical test was used which measures how poorly a fit of a theory is to a set of experimental results (Fessler & Ahn 2003). Chi Squared statistics was performed using software called Gnu plot which is a command line program that can perform data fit calculations. Further information can be found in the Gnu Plot 5.06 manual online.

9.4. Limitations and justifications

Limitations

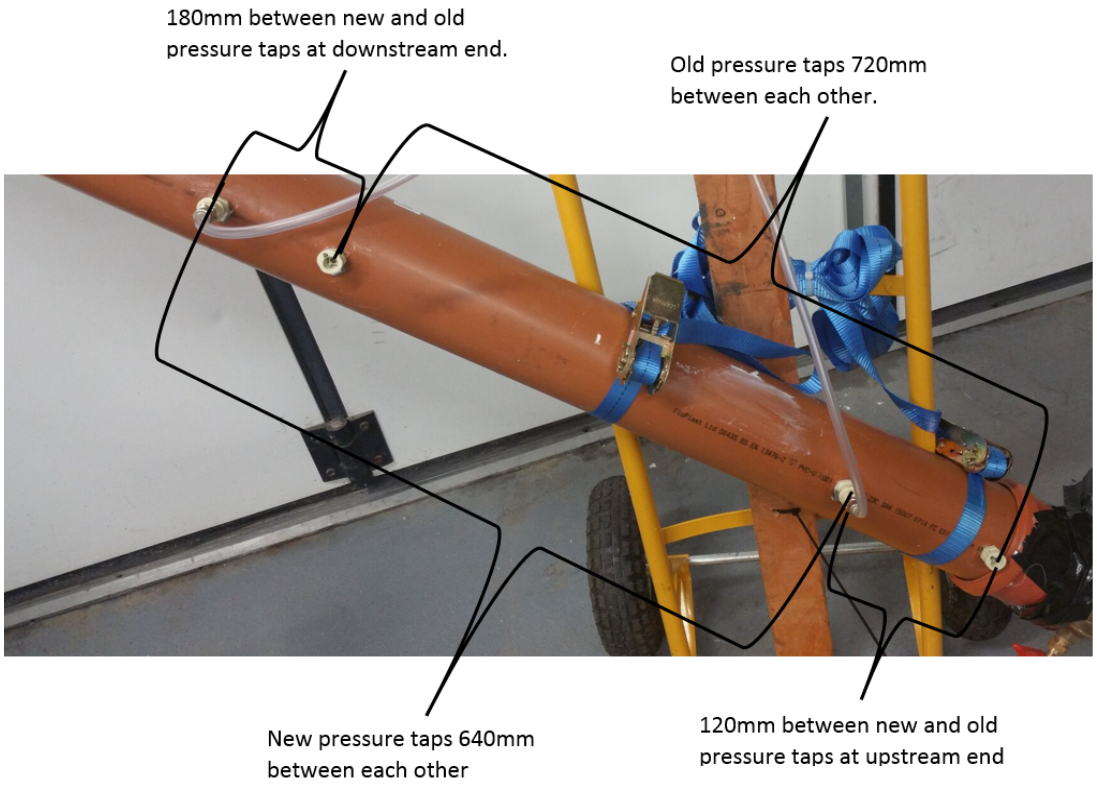

Figure-10: Pressure taps installed on the test pipe

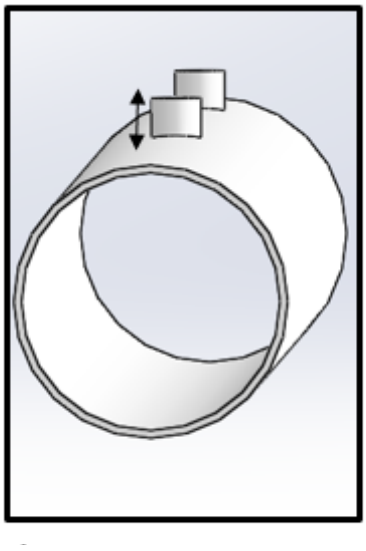

Figure-11: Pressure taps vertical to pipe.

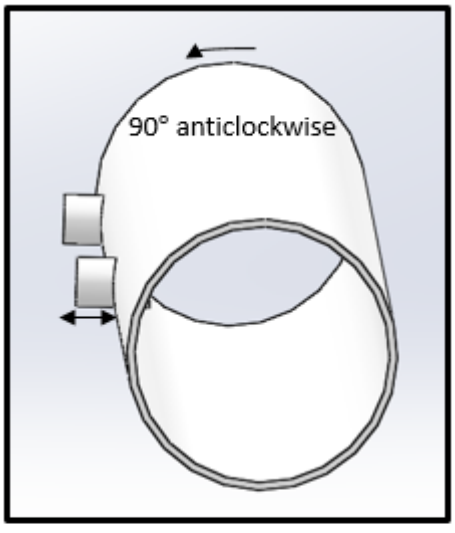

Figure-12 Pressure taps turned 90 degree anticlockwise to make it horizontal.

It was very hard to insert the topography properly inside the pipe and several attempts were required. The first attempt was done by rolling the topography and wrapping it

in a plastic film and then inserting it into the pipe. This method appeared to have worked well and the topography fitted well inside the pipe with the plastic film on the outer surface of the topography. A preliminary test with the topography in it pumped water into the pipe, but the topography was instantly shot out of the pipe. After analysing the reason it was found that the plastic film between the topography and the pipe wall contact point reduced the grip between the inner pipe wall and the topography. Although the topographic sheet was tacky and gripped, due to the plastic film wrapping it made the topography slippery. The rectangular topographic sheet when rolled and inserted into the pipe had a significantly big gap between each end of the sheet, which then made it impossible to study the whole circular topographic layer inside the pipe. If attempts were made to join each end of the sheet inside the pipe the whole diameter of the topographic roll reduced and would not sit properly on the pipe wall. Also, water might flow through the gap between the pipe wall and the topographic roll surface.

The pressure taps installed on the pipe did not respond properly because in the beginning the pipe was tightened to the trolley frame with the pressure taps vertically upwards as shown in Figure-11 on the pipe which reduced the amount of water entering the pressure tube through the tap. The pipe had to be turned 90° anticlockwise to make the pressure tap horizontal to the pipe, as shown in Figure-12, which increased the water flowing into the pressure tap. As shown in Figure 10, a pressure tap was installed 140mm above the downstream end of the topographic roll and another pressure tap was installed 720mm up from the downstream pressure tap on the upstream end of the topographic roll. The pressure taps had to be relocated up from their old position so two new pressure taps were installed. The downstream pressure tap was installed 180mm up from the old pressure tap and the upstream pressure tap was 120mm up from the old pressure tap.

Justification

The test went well without any failure on the test apparatus and enabled results to be obtained for the measured variables. The gap between the ends of the topographic roll was an advantage so that the pressure tap could fit in between the gap and contact the water which made the water enter the pressure tube efficiently. Turning the pipe 90° anticlockwise reduced the quantity of air bubbles inside the pressure tube. The test pipe was mounted 37° to the horizontal so that water would not shoot out a long distance, and the topography sat inside the pipe with the aid of gravity.

10. Results

A full table of the results is shown in Appendix-14.

10.1. Statistical results

10.1.1 Graph-1 plain pipe

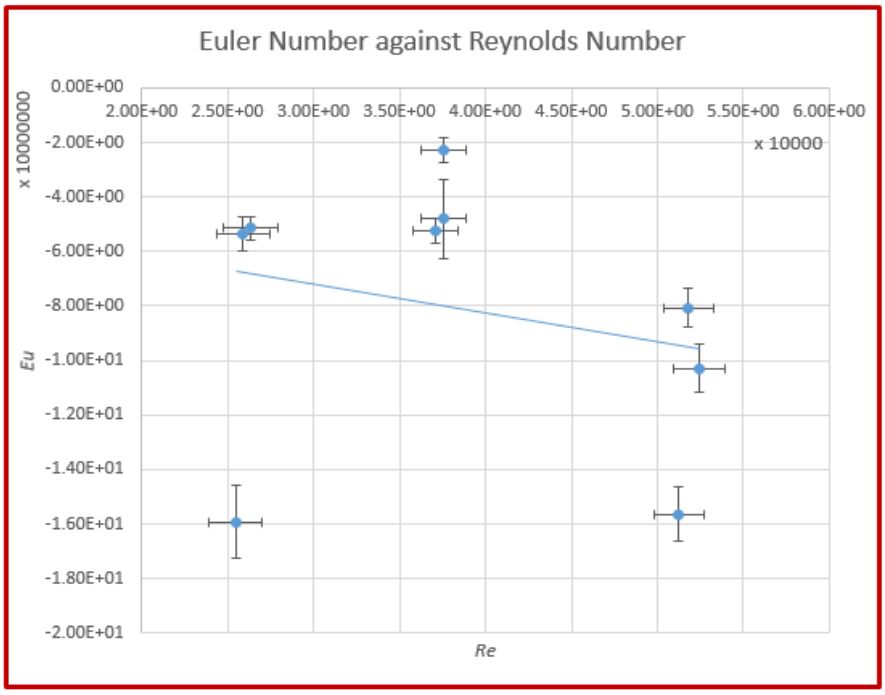

Figure-13: Graph of Euler number against Reynolds number from plain pipe test.

10.1.2. Graph-2 Topography-1

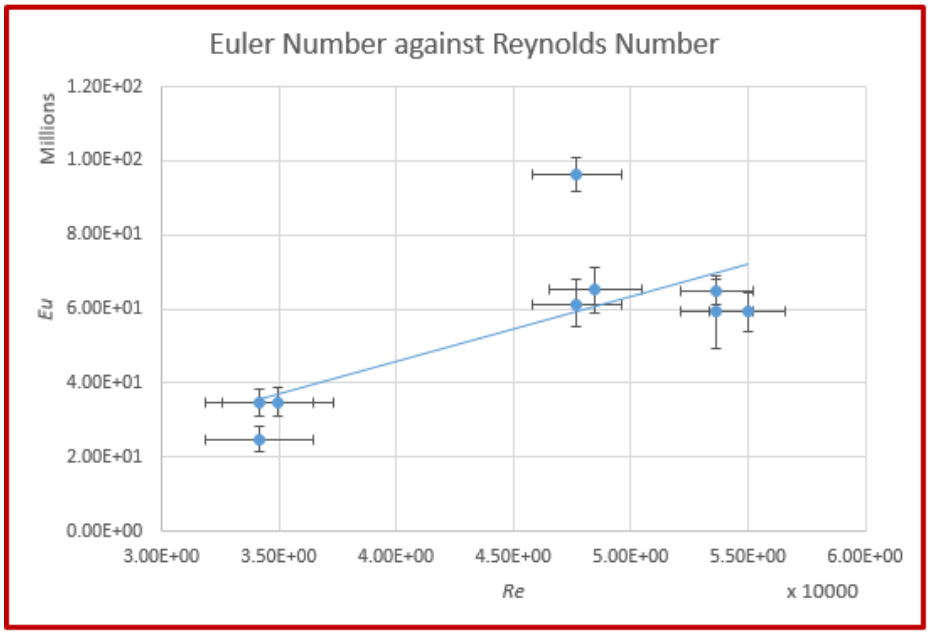

Figure-14: Graph of Euler number against Reynolds number from Topography-1 test.

10.1.3. Graph-3 Topography-2

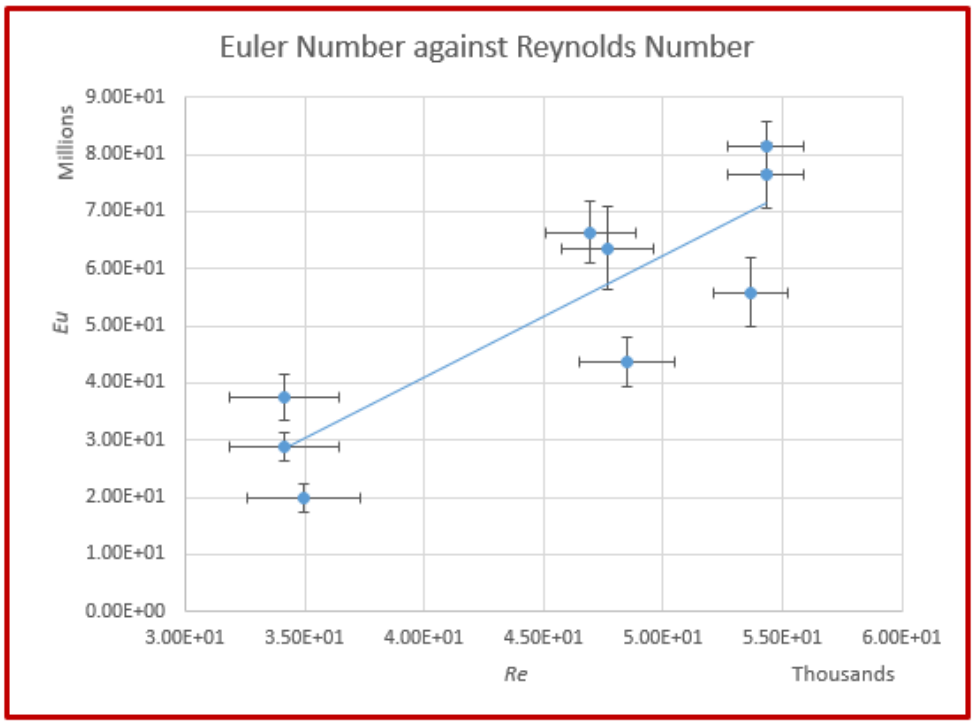

Figure-15: Graph of Euler number against Reynolds number from Topography-2 test.

10.1.4. Graph-4 Euler Number against Reynolds Number in all condition

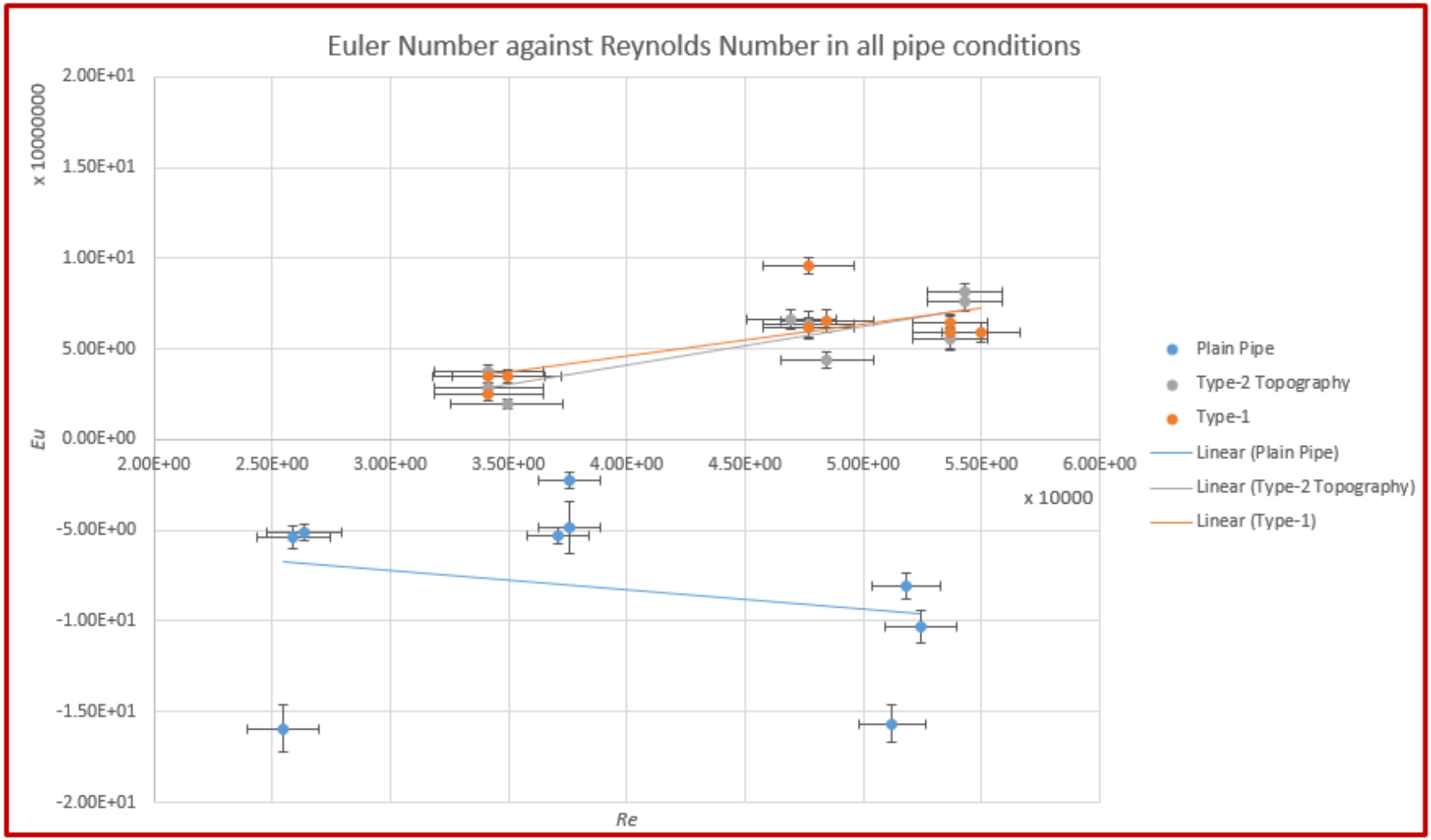

Figure-16: Graph of Euler number against Reynolds number in all pipe conditions.

10.1.5. Gnu plot result-1

```
After 21 iterations the fit converged.
final sum of squares of residuals : 960.291
rel. change during last iteration : -3.45091e-006

degrees of freedom    (FIT_NDF)                        : 7
rms of residuals      (FIT_STDFIT) = sqrt(WSSR/ndf)    : 11.7126
variance of residuals (reduced chisquare) = WSSR/ndf   : 137.184
p-value of the Chisq distribution (FIT_P)              : 0

Final set of parameters            Standard Deviation
=======================            ==========================
Adl             = -7897.9          +/- 1732         (21.93%)
Bdl             = 0.926083         +/- 0.2051       (22.15%)

correlation matrix of the fit parameters:
                Adl    Bdl
Adl             1.000
Bdl            -0.997  1.000
WARNING: Plotting with an 'unknown' terminal.
No output will be generated. Please select a terminal with 'set terminal'.
WARNING: Plotting with an 'unknown' terminal.
No output will be generated. Please select a terminal with 'set terminal'.
WARNING: Plotting with an 'unknown' terminal.
No output will be generated. Please select a terminal with 'set terminal'.
WARNING: Plotting with an 'unknown' terminal.
No output will be generated. Please select a terminal with 'set terminal'.
WARNING: Plotting with an 'unknown' terminal.
No output will be generated. Please select a terminal with 'set terminal'.
Ratio of posterior probability of model d to posterior probability of model s: 0.0
gnuplot> load "Smooth_pipe_two_conditions.gp"_
```

Figure-17: Command line section from the Gnu Plot program showing the probability ratio between model d and s.

10.1.6. Gnu plot result-2

```
After 26 iterations the fit converged.
final sum of squares of residuals : 669.823
rel. change during last iteration : -3.01374e-006

degrees of freedom    (FIT_NDF)                        : 7
rms of residuals      (FIT_STDFIT) = sqrt(WSSR/ndf)    : 9.78208
variance of residuals (reduced chisquare) = WSSR/ndf   : 95.689
p-value of the Chisq distribution (FIT_P)              : 0

Final set of parameters            Standard Deviation
=======================            ==========================
A               = -7390.84         +/- 1250         (16.92%)
B               = 0.93184          +/- 0.1589       (17.06%)

correlation matrix of the fit parameters:
                A      B
A               1.000
B              -0.995  1.000
WARNING: Plotting with an 'unknown' terminal.
No output will be generated. Please select a terminal with 'set terminal'.
WARNING: Plotting with an 'unknown' terminal.
No output will be generated. Please select a terminal with 'set terminal'.
Number of data points: 18.0
Marginal likelihood: {-1.28729068668779e-289, -7.16896733480647e-291}
Posterior expectation of A: -7390.8400025027
Posterior expectation of B: 0.931840348454348
Posterior standard deviation (standard error) of A: 1250.22946094273
Posterior standard deviation (standard error) of B: 0.158926950960006
gnuplot> _
```

Figure-18: Command line section from the Gnu Plot program showing the value expectation of constant A and B for both Topography-1 and Topography-2.

11. Discussion

11.1. Result discussion

The results collected from the experiment are water level difference, time taken for the water to reach the pre-set water level difference and finally the head difference of the pipe flow. Volume of water is calculated using equation-1 in the formula sheet shown in Appendix-13. Volume flow rate of the water flow is determined by using the calculated volume and the time taken using equation-2 in the formula sheet in Appendix-13. Equation-3 in the formula sheet is used to calculate the Reynolds number of the water flow. The Euler number is then calculated using equation-5 shown in Appendix-13. The standard deviation and standard error were also plotted on each Euler number against the Reynolds number graph, the equation for error equation used on the Euler number is shown in Appendix-13, Equations-7 and 8. The Reynolds number random error was calculated using the formula:

$$\varphi = \pm\sqrt{\left(\left(\frac{\partial Re}{\partial V}\times V_{error}\right)^2 + \left(\frac{\partial Re}{\partial t}\times t_{error}\right)^2\right)}$$ where $Re = \frac{4\rho V}{\pi D t \mu}$ as flow rate Q= V/t (Rossberg 2008).

The Chi Squared statistic is performed on Models s and d and Figure-17 shows the section of command lines from the Gnu plot test result. The black underlined command line shows the posterior probability of the model to be true. Posterior probability is said to be the statistical probability that a theoretical model is true from the relevant observation (MacKay 2003). The equation governing posterior probability which is applied in the Gnu Plot is shown in equation-10 in Appendix-13. The posterior probability ratio is the ratio between Model d and Model s. The statistical results show the posterior probability ratio is zero which means the probability of Model d is closer to zero and the probability of Model s is closer to 100% (Williams & Kelley 2017). Therefore, the result from the Gnu plot shows that the value of constants A and B is same for Topography-1 and 2.

Figure 18 shows the constants A and B value expectations and their standard deviation in Topography-1 and 2 Colebrook's equation. The value of A is about -7390.84 to 2 d.p and the value of B is about 0.93 to 2 d.p (Williams & Kelley 2017). The red underlined command lines show the standard deviation in calculating the expectation values of A and B; the standard deviation on constant A value is about $\pm$1250 (16.92%) and the standard deviation on constant B value is about $\pm$0.16 (17.1%) (Williams & Kelley 2017).

A graph of the Euler Number against the Reynolds number is plotted based on the plain pipe results and is shown in Figure 13. The graph shows a negative linear relationship between the Euler number and the Reynolds Number. The Euler number is based on the vector head difference (Joubert & Brown 1968); head difference is negative in the plain pipe. As the Reynolds number increases the Euler number decreases. The Euler number decreases as the Reynolds number increases like the pressure drop in circular pipes in laminar flow (Oakman & Liow 2016). The flow in the plain pipe is less turbulent than the topographic pipe (Tables 1 to 27, Appendix 14)

which means the plain pipe had a slightly laminar flow compared with Topography-1 and 2.

The reason for the negative head difference is because the water enters the test pipe from a 40mm diameter pipe reducer, as shown in Appendix-12 Figure 30. The pipe reducer has quite a small diameter compared to the test pipe diameter therefore there is a sudden expansion in the cross-section area as the water enters the test pipe. Increasing the cross-section of the water carrying section decreases the average flow velocity suddenly and therefore energy loss takes place hence total head decreases at the upstream head (Yinpeng, Changjin & Mingda 2015). Mammoli & Brebbia (2009) show the pressure difference reducing to negative due to a sudden enlargement. Δp is the static pressure and z/d is the axial position for sudden enlargement. The downstream end is not affected by this phenomenon because the downstream pressure tap lies 640mm away from the upstream pressure tap so by that distance the flow will recover from the effect of sudden expansion (Yinpeng, Changjin & Mingda 2015). This creates a negative overall head difference in the plain pipe flow.

There are some outliers on the plain pipe graph because there were a lot of random errors occurring during the experiment and while collecting the results on the measured variables. The reasons for the error sources are discussed below.

The second experiment was based on Topography-1. A graph of the Euler Number against the Reynolds Number is shown in Figure-14. The Topography-1 graph shows a positive linear trend between the Euler number and the Reynolds number. As the Reynolds number increases the Euler number also increases linearly. This also shows that the head difference increases as the Reynolds number increases. The higher Reynolds number causes a larger head difference at the stagnation point (Ramkissoon 1998). At the higher Reynolds number the viscous effect can be neglected and the inertial force predominates (Liptak 1993). Therefore, at the higher Reynolds number the head difference increases. As the water enters from the narrow section to the wide section of the pipe it quickly enters the topographic surface which creates a turbulent region. Turbulence occurs when the Reynolds number is high therefore the head at the upstream end of the topography is higher than the head at the downstream end. As the head increases the Euler number also increases as the latter is the ratio of the head difference and the inertial force (Khatsuria 2004).

The third test was the Topography-2 test. A Graph of the Euler number against the Reynolds number on Topography-2 is shown in Figure 15. Tables 19 to 27 in Appendix 14 shows the results of the Topography-2 test sets. Similarly to Topography-1, the graph shows a positive linear relation between the Euler number and the Reynolds number. As the Reynolds number increases the Euler number also increases.

Tables 1-18 show unexpected changes in the flow rate of the water in the pipe flow between the plain pipe and Topography-1. The Topography-2 flow rate shows a similar trend to Topography-1. The flow rate in the plain pipe is lower than the topographic pipes. The reason is leakage of the pipe connection between the pump and the test pipe, and that reduced the volume of water moving into the empty tank per time, and that affected the flow rate parameter calculated for the plain pipe experiment. The pipe was still leaking during Topography-1 and 2 testing even though it was fixed with duct tape.

The Euler number against the Reynolds number graph is shown in Figure 16 and clearly shows the difference in characteristics of the pipe flow with and without topography. The graph also shows that between Topography-1 and 2, Topography-2 has a greater effect than Topography-1 because Topography-2 has the bigger topographic asperities than Topography-1. Topographic asperities in type-2 are twice as big as topographic asperities of Topography-1.

11.2. Evaluation

11.2.1. Instrumentation

There were significant factors about the measuring instruments used which benefited the precision of the results gained. The stop watch used to measure the time taken was digital so that it displayed the exact numerical value of the time which improves the precision of the time value. The open top manometer was very sensitive as the meniscus in the pressure tubes fluctuate according to the changes of the flow characteristics.

Sources of error in instrumentation included, the meniscus in the pressure tube fluctuating irregularly and randomly which prevented precise visual observation of the head difference. Even though video recordings were made to read off the head difference value it didn't produce an expected and reasonable result. Quick pausing of the video at random times created blurry images to read off the head difference values and that gave an unreliable and inaccurate result.

The video camera had to be hand held to record the fluctuations of the meniscus in pressure. The camera was shaking slightly which made it hard to analyse the video recording of the head difference. The camera was not pointing directly above on the meniscus and that also caused parallax error.

To obtain the head difference value video playback was paused in 6 random play times. The head difference at those play times didn't look reasonable even though an average value was taken from 6 values.

11.2.2. Test condition

The water in the tank was oscillating severely due to unfavourable weather conditions so that there was a continuous fluctuating water level on the measuring ruler. This forced an estimate of the water level therefore leaving room for inaccuracy in time keeping. For example, when measuring the time of the water level dropping from 30cm to 20cm, oscillation caused recording from the ruler to be affected by the constant movement of the water; the amplitude of the oscillation is estimated to be maximum of $\pm$ 15% error. Error occurring in the test condition was accounted in the random error calculation.

11.2.3. Test model

The dimensions of the mold design were produced with tolerance of 0.1mm to the laser cutting machine; however, the machine cut out the mold with a tolerance of 0mm. The rubber solution was viscous therefore there were some limitation for the rubber solution to flow into the cylindrical slot in the mold. This might have contracted the diameter and depth of the cylindrical topography from the actual design to a small degree, which should be negligible. The topography was not rigid but flexible therefore when water flowed on it the topography might have bent along the direction

of the flow instead of staying rigid and blocking the flow, which may have produced inaccuracy in the results. The surface finish of the rubber was smooth and therefore its resistance against the water flow was unknown. The releasing of the topographic cast from its mold was very risky and the shape of the topographic asperities didn't come out as required. The test model error is not included in the statistical error calculations.

11.2.4. Human error

More than one variable result had to be measured at the same time i.e. water height difference, time taken to reach the height difference and then video recording the head difference. Therefore, chances for misreading the time value was high. The procedure of the whole variable measurement is explained in Appendix-2.

The time taken to reach the water level difference in the tank was not measured precisely due to the long reaction time, it was not possible to simultaneously start the stop watch at the same time as the pump is switched on.

The observations on water level difference were not done by looking directly at the ruler fixed in the tank, which produced inaccurate time values for each test run. Human error is incorporated in both the standard and random error calculations.

12. Conclusions

Generally, the experiment investigating the effect caused by the topography upon the water flow was successful and reliable, due to the instruments measuring the key variables. From the calculations undertaken based on the experimental results it can be concluded that topographies have some effect on the pipe flow. Increasing the size of the topography increases the head difference and turbulent flow therefore in this situation the pump needs to provide more power to the water flow to pump the water up to the next tank. The head difference is said to be the head loss therefore hydraulic energy loss. This study helps engineers to consider the topographic factors when they manufacture pipes, check for any design flaws and inspect for any small projections of the materials inside the pipe. Principles are proved by this study, particularly the valuable reductions in energy consumption, hence providing improvements to the quality of life in society generally.

13. Future recommendations

13.1. Manufacturability before designing

The manufacturability and setting up of the model properly needs to be researched and clarified before designing the actual model. Designing can be done easily using 3D simulation computer software but making the computer model into practical use may not always be possible or it may be expensive to manufacture the designed model. Design some simply shaped topography that can be manufactured to as low a budget as possible in the future.

13.2. Test conditions

Experimenting the topography inside Plymouth University's Marine building can avoid unfavorable weather conditions such as high winds and rain and hence obtain improved outcomes. Conduct all the test runs in the same day and in the same atmospheric condition to obtain reliable results.

13.3. Measuring instrument

A digital pressure gauge can be used to obtain accurate pressure differences hence head difference because, like the digital stop watch, a digital pressure gauge shows the exact numerical value of pressure differences. The fluctuation in the head difference will be relatively low therefore it will be easy to obtain the head difference accurately. However, the angle at which the test pipe is fixed needs to be considered as the digital pressure gauge does not consider this factor whereas an open top manometer does.

13.4. Test model and method

It should be ensured that the machine calibration is done before manufacturing the mold otherwise the tolerance requirement on the designed mold would not be met.

A stiffer casting material would prevent bending of the topographic asperities as water flows over them. Skewness and Kurtosis need to be analysed after obtaining the results as these two statistical tests would analyse the topographic features at a high level.

14. References

Afzal, N 2007, 'Friction Factor Directly From Transitional Roughness in a Turbulent Pipe Flow', *Journal of Fluid Engineering*, vol 129, no. 10, p. 1255.

Allen, JJ, Shockling, MA, Kunkel, GJ & Smits, AJ 2007, 'Turbulent flow in smooth and rough pipes', *Philosophical Transactions of The Royal Society*, vol 365, p. 701.

Bansal, RK 2001, *Mechanical Engineering (O.T.)*, 6th edn, Laxmi Publications (P) LTD, New Delhi.

Batchelor, GK 1955, 'On steady laminar flow with closed streamlines at large', Cambridge Core, Cambridge.

Brown, GO 2003, 'The History of the Darcy-Weisbach Equation for Pipe Flow Resistance', *ENVIRONMENTAL AND WATER RESOURCES HISTORY*, pp. 35,37 & 39.

Cengel, YA & Cimbala, JM 2013, *Fluid Mechanics Fundamentals and Applications (Mechanical Engineering)*, 3rd edn, McGraw-Hill Education, New York.

Chapman, S 2008, *Salters Horners Advanced Physics AS Student Book*, Pearson Education, Limited, Harlow.

Chasis, DA 1988, *Plastic Piping Systems*, 2nd edn, Industrial Press Inc., New York.

Clifford, M, Brooks, R, Howe , A, Kennedy, A, McWilliam, S, Pickering, S, Shayler, P & Shipway, P 2006, *An Introduction to Mechanical Engineering Part 1*, Taylor & Francis Group, Boca Raton, Florida.

Faber, TE 1995, *Fluid Mechanics for Physicists*, Cambridge University Press, Cambridge, UK.

Fessler, JA & Ahn, S 2003, 'Standard Errors of Mean, Variance, and Standard Deviation Estimator', The University of Michigan, Michigan.

Gordon, RA 2012, *Applied Statistics for the Social and Health Sciences*, Routledge Tylor & Francis Group, New York.

Hamill, L 2011, *Understanding Hydraulics*, 3rd edn, PALGRAVE MACMILLAN, Hampshire, UK.

Harimkar, Narendra, BD & Sandip, P 2008, *Laser Fabrication and Machining of Materials*, Springer Science+ Business Media.LLC, New York.

Jeffreys, H 1961, *THEORY OF PROBABILITY*, 3rd edn, Oxford University Press Inc., New York.

Jones, GM, Sanks, RL, Tchobanoglous, G & Bosserman ll, BE 2008, *Pumping Station Design: Revised 3rd Edition*, 3rd edn, Elsevier, Oxford, UK.

Joubert, PN & Brown, KC 1968, 'The measurement of skin friction in turbulent boundary layers with adverse pressure gradients', *Journal of Fluid Mechanics*, vol 35, no. 4, p. 756.

Judy, J, Maynes, D & Webb, BW 2002, 'Characterization of frictional pressure drop for liquid', *International Journal of Heat and Mass Transfer*, vol 45, p. 3486.

Kalyanaraman, D 2012, 'Industrial flow meters/flow transmitters', *Analog Applications Journal*, vol 2, p. 29.

Kandlikar, SG, Schmitt, D, Carrano, AL & Taylor, JB 2015, 'Characterization of surface roughness effects on pressure drop in single-phase flow in minichannels', Rochester Institute of Technology, New York.

Kartal, NS & Green, F 2002, 'Decay and termite resistance of medium density fibreboard (MDF) made from different wood species', *International Biodeterioration & Biodegradation*, vol 51, no. 2003, p. 29.

Khatsuria, RM 2004, *Hydraulics of Spillways and Energy Dissipators*, Taylor & Francis Group, Boca Raton, Florida.

Knezevic, D, Lovrec, D, Jocanovic, M & Karanovic, V 2009, 'Determination of Pressure Losses in Hydraulic Pipeline Systems by Considering Temperature and Pressure', *Journal of Mechanical Engineering* , vol 55, p. 238.

Li, X, Li, Y, Zhong, Z, Wang, D, Ratto, JA, Sheng, K & Sun, XS 2009, 'Mechanical and water soaking properties of medium density fiberboard with wood fibre and soybean protein adhesive', *Bioresource Technology*, vol 100, no. 2009, p. 3556.

Liptak, BG 1993, *Flow Measurment*, Chilton Book Company, Radnor, Pennsylvania.

MacKay, DCJ 2003, *Information theory, inference and learning algorithms*, Cambridge University Press, Cambridge.

Mammoli, AA & Brebbia, CA 2009, *Computational Methods in Multiphase Flow V*, WIT Press, Southampton, UK.

Mills, AF 1992, *Heat Transfer*, Richard D. Irwin, Inc, Concord, Massachusetts.

Mold Max® 60 High Heat Resistant Silicone Rubber Compound 2017, viewed 08 March 2017, <https://www.smooth-on.com/tb/files/MOLD_MAX_60_TB.PDF>.

Munson, BR, Young, DF, Okiishi, TH & Huebsch, WW 2010, *Fundamentals Of Fluid Mechanics*, 6th edn, John Wiley & Sons Inc., Hoboken, New Jersey.

Oakman, OA & Liow, JL 2016, 'Simulation and Experimental Validation of an Axial-Flow Hydrocyclone', School of Engineering and Information Technology, Perth.

Ramkissoon, H 1998, *IUTAM Symposium on Lubricated Transport of Viscous Materials*, Springer Science+Business Media B.V, Dordrecht, Netherlands.

Romeo, E, Royo, C & Monzon, A 2001, 'Improved explicit equations for estimation of the friction factor in rough and smooth pipe', *Chemical Engineering Journal*, vol 86, no. 2002, p. 369.

Rossberg, AG 2008, 'LAPLACE TRANSFORMS OF PROBABILITY DISTRIBUTIONS AND THIER INVERSIONS ARE EASY ON LOGARITHMIC SCALES', *Journal of Applied Probability*, vol 45, no. 2, p. 5.

Shenoy, GV, Srivastava, UK & Sharma, SC 2002, *Business Statistics*, New Age International (P) Limited, Publishers, Delhi.

She, ZS, Wu, Y, Chen, X & Hussain, F 2012, 'A multi-state description of roughness effects', *New Journal of Physics*, vol 14, p. 13.

Shockling, MA, Allen, JJ & Smits, AJ 2006, 'Roughness effects in turbulent pipe flow', Cambridge University Press, Cambridge.

Smith, EH 1994, *Mechanical Engineer's Reference Book*, 12th edn, Butterworth-Heinemann Ltd, Oxford.

Sonnad, JR & Goudar, CT 2007, 'Explicit Reformulation of the Colebrook-White Equation for Turbulent Flow Friction Factor Calculation', *American Chemical Society*, vol 46, p. 2593.

Squires, GL 2001, *Practical Physics*, 4th edn, Cambridge University Press, Cambridge.

Walshin, M 1960, *SUBMERSIBLE PUMP*, New York, USA, viewed 22 April 2017, <https://docs.google.com/viewer?url=patentimages.storage.googleapis.com/pdfs/US2927174.pdf>.

Williams, T & Kelley, C 2017, *Gnu Plot* (5.06) [Computer program]. Downloaded 24 April 2017, < https://sourceforge.net/projects/gnuplot/>.

Yang, JT, Chen, CK, Tsai, KJ, Lin, WZ & Sheen, HJ 2007, 'A novel fluidic oscillator incorporating step-shaped attachment walls', *Sensors and Actuators*, vol 135, p. 482.

Yinpeng, L, Changjin, W & Mingda, H 2015, 'Discussion on Local Resistance Coefficient of Sudden Expansion Pipe', *Journal of Applied Science and Engineering Innovation*, vol 2, no. 2, p. 38.

Appendices can be seen in Supplementary files in the list of Article Tools showing to the right-hand side of the main window.